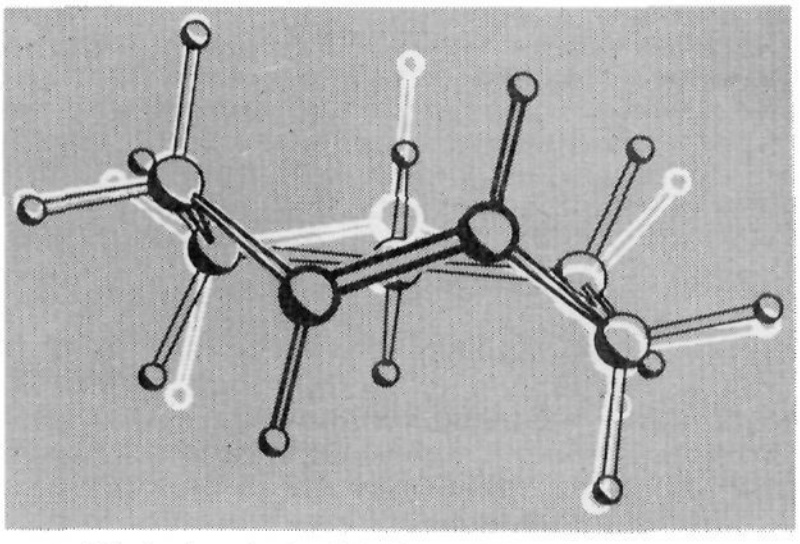

Figure 8. Black: the calculated (MOLBD III) transition-state geometry for the pseudorotation of free *trans*-cycloheptene. White: the geometry reached from the transition state upon displacement in the direction of the reaction coordinate (the normal mode with imaginary frequency).

superimposed structures indicate the direction of motion along the reaction coordinate at the transition state, i.e., the one normal mode of the transition state which has a negative force constant.

Conclusions

The ^{13}C DNMR behavior of the CuOTf complex of *trans*-cycloheptene shows that the equilibrium geometry of the olefin has no symmetry elements. The results of molecular mechanics and semiempirical quantum mechanical calculations show free *t*-C_7H_{12} to have an unsymmetrical chair equilibrium geometry.

It is proposed that the observed dynamical process is due to conformational automerization (pseudorotation) of the olefin. The calculated $\Delta G^{\ddagger}$ values for the automerization of the free olefin are 10.5 and 8.6 kcal/mol, using MOLBD and MNDO, respectively. They are in excellent agreement with the experimental value of 9.47 ± 0.20 kcal/mol found for *t*-C_7H_{12}·CuOTf at 299 °C, particularly in view of the fact that quantum mechanical calculations of this type are known generally to underestimate activation barriers.[22,30a] In principle, the agreement may be only apparent in that the calculation is on the free olefin and the measurement on a complexed olefin. As noted above, however, extrapolation of previous experience with similar olefins and complexes suggests strongly that the effects of the complexation on conformational mobility of the cycloalkenes are minor.

Experimental Section

The cycloalkene complexes were prepared according to ref 12 and 13. The ^{13}C NMR spectra were run on a Varian SC-300 spectrometer using dried, degassed diethyl ether as solvent. The probe temperature was calibrated with a ^{13}C chemical shift thermometer and has an absolute uncertainty of ±1°C at the lowest temperature. The line-shape analysis employed a program based on the method of Nakagawa.[33] The error limits in the rate constants were taken from simulated spectra corresponding to values which are clearly either too fast or too slow based on visual fitting. The values of the free energy of activation were calculated from the Eyring equation, $\Delta G^{\ddagger}$ (cal mol^{-1}) = $1.9872T(23.7600 + \ln T - \ln k)$. The DNMR kinetic data for *t*-C_7H_{12}·CuOTf and *c*-C_8H_{14}·CuOTf are presented in the table.

The molecular mechanics calculations used the MOLBD III program[16] with modifications similar to those reported in ref 31. The MNDO calculation was done using the standard program of Dewar.[17]

Acknowledgment is made to the donors of the Petroleum Research Fund, administered by the American Chemical Society, for the support of this research (PRF 13172-AC4,6), and to the University of Utah for a research fellowship to G.M.W. The authors thank Dr. J. W. Downing and Mr. K. A. Klingensmith for assistance in the computational aspects of this work. Useful discussions with Dr. Eric Johnston are also gratefully acknowledged, as is the communication of unpublished results by Professor D. Dougherty (California Institute of Technology).

Registry No. 2, 69515-66-8; **3**, 69496-00-0; **5**, 85761-20-2; **7**, 51826-48-3; **8**, 85735-19-9.

(33) Nakagawa, T. *Bull. Chem. Soc. Jpn.* **1966**, *39*, 1006.

Study of Electron Distributions of Molecular Orbitals by Penning Ionization Electron Spectroscopy

Koichi Ohno,* Hideki Mutoh, and Yoshiya Harada

Contribution from the Department of Chemistry, College of General Education, The University of Tokyo, Komaba, Meguro-ku, Tokyo 153, Japan. *Received August 2, 1982*

Abstract: Penning ionization electron spectroscopy (PIES) has been used to study spatial electron distributions of individual molecular orbitals. On the basis of comparison of observed band intensities with electron densities of ab initio molecular orbitals, a simple principle for orbital activities in Penning ionization has been established; the outer orbital which is exposed outside the van der Waals surface is active and the inner orbital which is localized inside the van der Waals surface is inactive. Penning ionization can be considered as an electrophilic reaction of rare gas atoms in metastable states with sample molecules. It is concluded that PIES is a sensitive method for probing orbital electron densities at the very frontier of the molecule where the molecule is attacked by the reagent.

The concept of the molecular orbital (MO) stems from the early days of the quantum theory. Its importance has been supported by a vast accumulation of experimental results and also by successful applications of quantum chemical methods to various problems. Although molecular orbitals are introduced on purely theoretical grounds, recent developments in photoelectron spectroscopy have made it possible to relate molecular orbitals to observed ionization bands for most closed-shell molecules.[1-3] Further, observed ionization potentials can be compared with theoretical orbital energies in many cases where Koopmans' theorem[4] is valid. This enables us to consider that individual electron energy levels in molecules can be observed experimentally. On the other hand, phenomena, which directly reflect orbital functions for "individual" molecular orbitals, have eluded observation hitherto, although "total" electron densities have been

(1) Siegbahn, K.; Nordling, C.; Fahlman, A.; Nordberg, R.; Hamrin, K.; Hedman, J.; Johansson, G.; Bergmark, T.; Karlsson, S.-E.; Lindgren, I.; Lindberg, B. "ESCA-Atomic, Molecular and Solid State Structure Studied by Means of Electron Spectroscopy"; North-Holland Publishing Co.: Amsterdam-London, 1967; Ser. IV, Vol. 20.

(2) Turner, D. W.; Baker, C.; Brundle, C. R. "Molecular Photoelectron Spectroscopy"; Wiley: New York, 1970.

(3) Kimura, K.; Katsumata, S.; Achiba, Y.; Yamazaki, T.; Iwata, S. "Handbook of He I Photoelectron Spectra of Fundamental Organic Molecules"; Japan Scientific Societies Press: Tokyo, 1981.

(4) Koopmans, T. *Physica (Amsterdam)* **1933**, *1*, 104–113.

0002-7863/83/1505-4555$01.50/0

measured by diffraction methods.

Branching ratios for the population of different ionic states produced upon ionization of molecules can be measured as relative partial ionization cross sections by electron spectroscopic methods.[5-7] In most closed-shell molecules, these quantities are proportional to probabilities for processes extracting electrons from individual molecular orbitals. Therefore, electron spectroscopic studies may provide information about individual molecular orbital functions.

Partial photoionization cross sections can be measured by photoelectron spectroscopy as functions of the photon energy. Angle-resolved studies provide further information about differential cross sections. Partial photoionization cross sections depend mostly on the types of atomic orbitals that constitute molecular orbitals. It is well known that the relative band intensities in photoelectron spectra are nearly the same when the comparison is made between ionizations from molecular orbitals that are made up from the same set of atomic orbitals.[7] Therefore, it is very difficult to obtain direct experimental information about spatial electron distributions of molecular orbitals from photoelectron spectroscopic studies.

In (e,2e) electron spectroscopy, electron distributions in the momentum space can be determined for individual molecular orbitals.[8-10] This technique has been used to estimate the quality of basis sets for MO calculations. However, the comparison has been made between theory and experiment for the electron distribution obtained as a function of the absolute value of the momentum. This means that the local character of orbitals in real coordinate space, which is important from the chemical point of view, cannot be considered directly in the (e,2e) technique. The relatively low resolution of about 2 eV in (e,2e) spectroscopy is a serious obstacle for its application to large molecules, because deconvolution of overlapping bands is necessary to obtain the momentum distributions.

Large differences were observed for the relative partial ionization cross sections of various molecules when UV photoelectron spectra (UPS) and Penning ionization electron spectra (PIES) were compared.[11-24] In PIES of polyatomic molecules, an enhanced ionization probability was observed for lone-pair electrons located on the N atom of the molecules containing the CN group.[11]

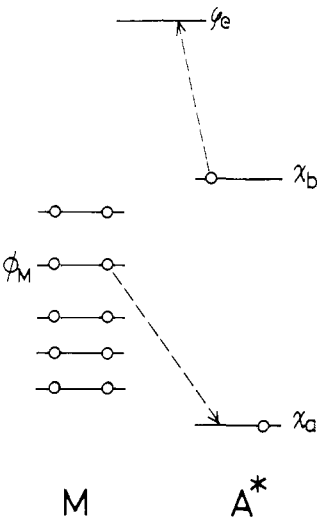

Figure 1. The electron-transfer process in Penning ionization. The metastable atom (A*) reacts as an electrophilic reagent with the sample molecule (M). An electron in a molecular orbital (ϕ_M) is transferred into the vacant inner-shell orbital (χ_a) of the metastable atom and an electron is ejected from the occupied outer-shell orbital (χ_b) of the metastable atom into the orbital (φ_e) of a continuum state.

For unsaturated hydrocarbons, the π bands in the PIES were found to be enhanced with respect to the σ bands in comparison with the UPS, and this finding was interpreted on the assumption that the transition probability depends on the electron distribution of molecular orbitals.[12] In subsequent studies of other unsaturated molecules, the spatial electron distribution of individual molecular orbitals has been indicated to be one of the most important factors governing the PIES intensity.[13,14]

The purpose of the present study is to establish a simple principle governing the PIES intensity on the basis of comparison between theoretical electron distributions of molecular orbitals and experimental band intensities. He I UPS and He*(2^3S) PIES were measured for some simple molecules by means of a transmission-corrected electron spectrometer. Electron distributions of molecular orbitals were calculated by an ab initio MO method with a 4-31G basis set. The nature of PIES was found to be very useful for probing spatial electron distributions of individual molecular orbitals at the very frontier of the molecule where the molecule is attacked by the reagent.

A Simple Model for Penning Ionization

When a molecule (M) meets with an excited atom (A*) with enough energy, an electron-transfer process can occur to yield an ionic state of the molecule (M^+) and the ground state of the atom (A) together with an ejected electron (e^-): $A^* + M \rightarrow A + M^+ + e^-$. Analysis of the kinetic energy distribution of the ejected electrons provides a Penning ionization electron spectrum (PIES),[25] which is similar in many respects to a UV photoelectron spectrum (UPS). Observed bands in both spectra are assigned to electrons in molecular orbitals for the usual closed-shell molecules. Kinetic energies of ejected electrons ($^1/_2mv^2$) can be related to ionization potentials (IP) which are equal to the absolute values of the orbital energies in Koopmans' theorem: $^1/_2mv^2 = E - IP - \delta$, where E is the energy of the excited atom or the photon and δ is the energy balance arising from relative motions among the particles. For UPS δ is negligible, whereas for PIES δ is a variable quantity depending on the distance between the excited atom and the target molecule where the electronic transition occurs. The variation of this quantity around the most effective distance may result in obscured vibrational structures. However, since the value of δ for PIES is usually not very large and much less than a few hundred meV, UPS and PIES are very similar in their energy scales. On the other hand, a considerable difference in the relative band intensities has been observed between UPS and PIES. This

(5) Baker, A. D.; Brundle, C. R. "Electron Spectrospectroscopy"; Academic Press: New York, 1977; Vol. 1, pp 1-73.
(6) Rabalais, J. W. "Principles of Ultraviolet Photoelectron Spectroscopy"; John Wiley & Sons: New York, 1977.
(7) Eland, J. H. D. "Photoelectron Spectroscopy"; Butterworths: London, 1974.
(8) Dixon, A. J.; Dey, S.; McCarthy, I. E.; Weigold, E.; Williams, G. R. J. *Chem. Phys.* **1977**, *21*, 81-87.
(9) Brion, C. E.; Hood, S. T.; Suzuki, I. H.; Weigold, E.; Williams, G. R. J. *J. Electron Spectrosc. Relat. Phenom.* **1980**, *21*, 71-91.
(10) McCarthy, I. E.; Weigold, E. *Endeavour* **1978**, *2*, 72-79.
(11) Čermák, V.; Yencha, A. J. *J. Electron Spectrosc. Relat. Phenom.* **1976**, *8*, 109-121.
(12) Munakata, T.; Kuchitsu, K.; Harada, Y. *Chem. Phys. Lett.* **1979**, *64*, 409-412.
(13) Munakata, T.; Ohno, K.; Harada, Y. *J. Chem. Phys.* **1980**, *72*, 2880-2881.
(14) Munakata, T.; Kuchitsu, K.; Harada, Y. *J. Electron Spectrosc. Relat. Phenom.* **1980**, *20*, 235-244.
(15) Kubota, H.; Munakata, T.; Hirooka, T.; Kuchitsu, K.; Harada, Y. *Chem. Phys. Lett.* **1980**, *74*, 409-412.
(16) Munakata, T.; Ohno, K.; Harada, Y.; Kuchitsu, K. *Chem. Phys. Lett.* **1981**, *83*, 243-245.
(17) Munakata, T.; Harada, Y.; Ohno, K.; Kuchitsu, K. *Chem. Phys. Lett.* **1981**, *84*, 6-8.
(18) Ohno, K.; Fujisawa, S.; Mutoh, H.; Harada, Y. *J. Phys. Chem.* **1982**, *86*, 440-441.
(19) Ohno, K.; Mutoh, H.; Harada, Y. *Surf. Sci.* **1981**, *115*, L128-L132.
(20) Yee, D. S. C.; Stewart, W. B.; McDowell, C. A.; Brion, C. E. *J. Electron Spectrosc. Relat. Phenom.* **1975**, *7*, 93-117.
(21) Yee, D. S. C.; Stewart, W. B.; McDowell, C. A.; Brion, C. E. *J. Electron Spectrosc. Relat. Phenom.* **1975**, *7*, 377-383.
(22) Yee, D. S. C.; Hamnett, A.; Brion, C. E. *J. Electron Spectrosc. Relat. Phenom.* **1976**, *8*, 291-312.
(23) Yee, D. S. C.; Brion, C. E. *J. Electron Spectrosc. Relat. Phenom.* **1976**, *8*, 313-323.
(24) Hotop, H.; Hübler, G. *J. Electron Spectrosc. Relat. Phenom.* **1977**, *11*, 101-121.
(25) Čermák, V. *J. Chem. Phys.* **1966**, *44*, 3781-3786.

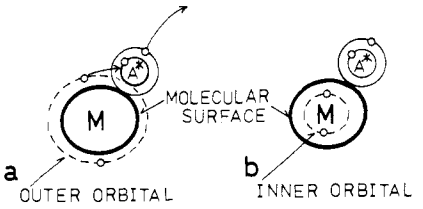

Figure 2. The principle for orbital activities in Penning ionization. The metastable atom (A*) can approach the molecule (M) up to the molecular surface shown by the solid curve. Electron transfer from M to A* can take place easily for the outer orbital (a) which has a large overlap with the vacant inner-shell orbital of A*. The process is almost forbidden for the inner orbital (b) because of its small overlap with the orbital of A* even when the metastable atom (A*) comes up to the minimum distance.

must be ascribed to the difference in the mechanisms between photoionization and Penning ionization.

Although the quantum-mechanical treatment of Penning ionization has been developed for atoms,[26-28] applications of such a treatment to large molecules are not so straightforward. Penning ionization involving a closed-shell ground-state molecule (M) and a metastable atom in an excited triplet state (^{3}A*) has been considered as an electron-transfer process,[29,30] which is schematically shown in Figure 1; an electron in a molecular orbital ϕ_M is transferred into the vacant inner-shell orbital χ_a of the metastable atom and followed by removal of an electron from the occupied outer-shell orbital χ_b of the metastable atom to yield an electron in a continuum state φ_e. The transition probability of this process is governed by an exchange-type interaction:

$$K = |\langle \chi_b(1)\phi_M(2)|(1/r_{12})|\varphi_e(1)\chi_a(2)\rangle|^2$$

The value of K increases exponentially as the metastable atom approaches the target molecule. This means that the most favorable distance for the transition must be in the neighborhood of the classical turning point of the collision trajectory, which occurs near the van der Waals surface where the interaction potential becomes repulsive. Furthermore, major contributions to the integral can be attributed to local regions where ϕ_M effectively overlaps with χ_a. Therefore, relative activities of individual orbitals are governed by electron densities of ϕ_M in the exterior region outside the van der Waals surface.

A clear insight is obtained for qualitative understanding when we imagine a classical collision between the metastable atom and the target molecule. The solid curve in Figure 2 indicates the boundary of the repulsive interaction between the metastable atom and the molecule. The dashed curve in Figure 2a shows an orbital extending out of the repulsive molecular surface, and the dashed curve in Figure 2b shows an orbital enveloped in the surface. Since an orbital exposed to the outside more easily interacts with incoming species, the outer orbital (a) overlapping the A* inner-shell orbital gives rise to a larger intensity in PIES than does the inner orbital (b). This provides an approximate selection rule for PIES; the outer MO which is exposed to the outside is active and the inner MO which is localized in the inside is inactive. Such an effect may be summarized as a stereoelectronic effect of molecular orbitals on Penning ionization.

Calculations

In order to verify the approximate selection rule for Penning ionization, theoretical orbital electron densities were calculated by the ab initio MO method with a 4-31G basis set[31] and the results were compared with the experimental PIES band intensities. For the qualitative comparison between the electron distribution and the PIES intensity, electron density maps were drawn. The repulsive molecular surfaces were estimated from the van der Waals radii of the atoms (r_C = 1.7 Å, r_O = 1.4 Å, r_N = 1.5 Å, r_H = 1.2 Å). The repulsive surface so obtained corresponds to the Stuart model[32] composed of spheres with the van der Waals radii. For a more quantitative comparison, total densities of electrons outside the repulsive molecular surface were defined as "exterior electron densities (EED)". The EED's were found to be in the range 0.01–0.10 for each orbital. Contributions due to the outer region over 1.5 Å from the van der Waals surface were neglected to save computation time, since these contributions were estimated to be less than 10^{-4}.

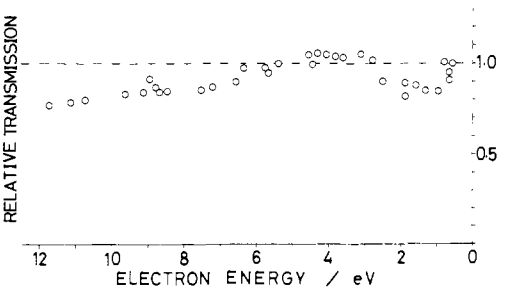

Figure 3. Energy dependence of the relative transmission of the electron spectrometer.

Experimental Section

The helium metastable atoms, 2^3S (19.82 eV) and 2^1S (20.62 eV), were produced by impact of 60-eV electrons with the beams of helium atoms collimated through a fused glass-capillary array. At this impact energy, the He I photons (21.22 eV) from the 2^1P state are negligible. A water-cooled helium discharge lamp was used as a quench lamp to eliminate 2^1S atoms, and almost pure (more than 95%) 2^3S atoms were introduced into the interaction chamber. The He I resonance line (584 Å, 21.22 eV) used for UPS was produced by a dc discharge in pure helium gas. The electron spectra were obtained at an ejection angle 90° with respect to the metastable atom beam or the photon beam by means of a hemispherical type analyzer with electron lens systems and scanning electrodes. The analyzed electrons were detected by an electron multiplier (Mullard B419BL) and a conventional pulse counter combined with a signal averaging system. Typical times for the measurements were about 60 min for UPS and 120 min for PIES. The energy dependence of the transmission of the electron spectrometer was determined by a detailed study of the UPS of O_2, CO, CO_2, N_2, C_2H_4, butadiene, and benzene. We compared our results with those of Samson and Gardner[33] and Kimura and co-workers.[3] As can be seen in Figure 3, the relative transmission efficiency is a smooth function of energy except for very small electron energies less than 0.5 eV.

Results

Figures 4–10 show the transmission-corrected He*(2^3S) PIES and He I UPS of NH_3, H_2O, H_2S, N_2, CO, C_2H_2, and C_6H_6. The observed bands are assigned to electrons in molecular orbitals. Electron density maps obtained by ab initio MO calculations with a 4-31G basis set are shown also in Figures 4–10. The thick solid curves in the maps indicate the molecular surfaces estimated from the van der Walls radii of the atoms. Since the real repulsive surface will not have such dips as shown in the figures, more appropriate surfaces are indicated for simple diatomic molecules by dashed curves (Figures 7 and 8). Contour lines of orbital electron densities are shown for a plane including the molecular symmetry axis, except for benzene. The contour lines for benzene (Figure 10) are shown for a plane 1.7 Å above the molecular plane.

Table I shows relative orbital activities (OA, α) in Penning ionization and exterior electron densities (EED, ρ_{calcd}) for the molecular orbitals concerned. The calculated EED (ρ) were found to be between 10^{-2} and 10^{-1}. This means that the electron density outside the molecular surface is only 1–10% for each orbital. The observed OA (α_{obsd}) was obtained for each MO from the observed He*(2^3S) PIES intensity. For degenerate orbitals, the integrated

(26) Nakamura, H. *J. Phys. Soc. Jpn.* **1969**, *26*, 1473–1479.
(27) Miller, W. H. *J. Chem. Phys.* **1970**, *52*, 3563–3572.
(28) Miller, W. H.; Slocomb, C. A.; Schaefer, H. F., III *J. Chem. Phys.* **1972**, *56*, 1347–1359.
(29) Hotop, H.; Niehaus, A. *Z. Phys.* **1969**, *228*, 68–88.
(30) Miller, W. H.; Morgner, H. *J. Chem. Phys.* **1977**, *67*, 4923–4930.
(31) Ditchfield, R.; Hehre, W. J.; Pople, J. A. *J. Chem. Phys.* **1971**, *54*, 724–728.
(32) Fieser, S.; Fieser, M. "Basic Organic Chemistry"; D. C. Heath: Boston, 1959; pp 13 and 14.
(33) Gardner, J. L.; Samson, J. A. R. *J. Electron Spectrosc. Relat. Phenom.* **1976**, *8*, 469–474.

band intensity was divided by the degeneracy, in order to make this quantity represent the orbital activity. Theoretical values of relative orbital activities were calculated from EED values and are shown in brackets (α_{calcd}). The α_{calcd} for N_2 and CO were obtained from ρ_{calcd} for the corrected molecular surface without dips (dashed curves in Figures 7 and 8). The values of α were normalized to the value of the most active MO.

Our experimental results can be compared with earlier results. Brion et al. have measured He* PIES of NH_3, H_2O, N_2, and CO.[20-22] Čermák et al. reported He* PIES of H_2O, H_2S, and CO.[34,35] Hotop et al. studied He* PIES of N_2 and CO.[24,36,37] Their results, however, have involved some problems. The metastable helium atom beam used by Brion et al. was contaminated with a large amount of He*(2^1S) atoms in addition to He*(2^3S) atoms. The energy sources used by Čermák et al. involved He I resonance photons as well as He*(2^3S) and He*(2^1S) atoms. Their He* PIES are therefore complicated, and analysis for the He*(2^3S) PIES intensities is difficult. In our results, contributions from He*(2^1S) or He I resonance photons are found to be negligible. It must be noted that band structures are much more resolved in our PIES of NH_3 and H_2O in comparison with those obtained by Brion et al.[21,22] Another problem is a very large background which significantly limits the accuracy of the intensity measurements. This makes earlier results less reliable for the analysis of the PIES intensities, especially for small electron energies less than 2 eV. The most serious cases are the lack of the third band of $H_2O(1b_2)$ and the third band of $CO(4\sigma)$ in earlier PIES. In our PIES, these bands have been observed in the very small energy region owing to a small background.

Ne* PIES of C_2H_2 and C_6H_6 were reported by Čermák.[38] The He* (2^3S) PIES of these molecules obtained in the present study show considerably improved aspects; structures are more resolved for the wider energy region and relative band intensities can be obtained more precisely.

Hotop et al. studied PIES of N_2 in detail and compared relative populations of produced ionic states with those measured in earlier work.[37] Their results were found to be different from those obtained by Brion et al.[20] The reason for this has been considered to be due to the difference in the methods of producing metastable atoms. Hotop et al. used a gas discharge, while Brion et al. used an electron gun. Hotop et al. pointed out that the difference in relative PIES intensities can be attributed to the difference in the average temperature of the metastable atom beams. Although we used the electron impact method as Brion et al. did, the relative PIES intensities of N_2 obtained in our experiments agreed with those for the metastable atom beams of 400 K obtained by Hotop et al. This may indicate that our metastable atom beams have an average temperature of about 400 K.

Discussion

In the PIES in Figures 4–6, bands due to electrons in the nonbonding orbitals ($3a_1$ orbital of NH_3, $1b_1$ and $3a_1$ orbitals of H_2O, $2b_1$ and $5a_1$ orbitals of H_2S) are much more enhanced than those due to electrons in the bonding orbitals. This can be explained qualitatively from the electron density maps. For example, the nonbonding orbital of ammonia ($3a_1$) has a large density outside of the molecular surface, whereas for the bonding orbital (1e) a smaller density is seen in the corresponding region. Necessarily, the nonbonding orbital is more active in PIES than the bonding orbital, since the orbital exposed to the outside has a larger overlap with the inner-shell orbital of the metastable atom. The same can be seen for water and hydrogen sulfide; the b_1- and a_1-type orbitals, which have nonbonding p-type character, are active in PIES, and the b_2 orbitals localized on the σ bonds are less active. These results clearly support the approximate selection rule for PIES proposed in the present study. For the UPS, no such simple relationship can be found between the spectral intensity and the spatial distribution of the orbital.

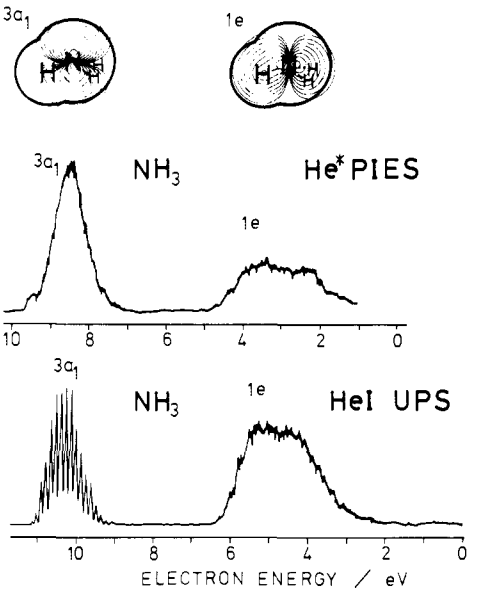

Figure 4. Transmission-corrected He* (2^3S) Penning ionization electron spectrum (PIES, upper) and He I photoelectron spectrum (UPS, lower) for NH_3. Electron density maps are shown for the relevant molecular orbitals. The density of the nth line from the outside (d_n) is $5 \times 2^n \times 10^{-4}$ au^{-3}.

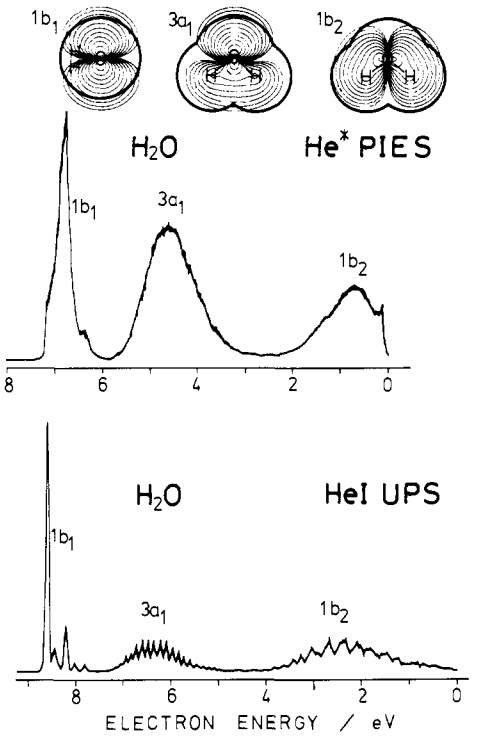

Figure 5. Transmission-corrected He*(2^3S) Penning ionization electron spectrum (PIES, upper) and He I photoelectron spectrum (UPS, lower) for H_2O, and electron density maps for the relevant molecular orbitals ($d_n = 2.5 \times 2^n \times 10^{-4}$ au^{-3}). A small peak at nearly 0 eV in the PIES is due to low-energy scattered electrons.

Although N_2, CO, and C_2H_2 are linear molecules of isoelectronic systems having two σ and one degenerate π orbitals, their PIES activities are considerably different (Figures 7–9, Table I); the relative order of the activity is $\sigma > \pi$ for N_2 and CO, whereas it is $\pi > \sigma$ for C_2H_2. This indicates that the symmetry of the orbitals is not necessarily correlated with the selection rule. The electron density maps in Figures 7–9 show the importance of the

(34) Čermák, V.; Yencha, A. J. *J. Electron Spectrosc. Relat. Phenom.* **1977**, *11*, 67–73.
(35) Čermák, V. *J. Electron Spectrosc. Relat. Phenom.* **1976**, *9*, 419–439.
(36) Hotop, H.; Niehaus, A. *Int. J. Mass Spectrom. Ion Phys.* **1970**, *5*, 415–441.
(37) Hotop, H.; Kolb, E.; Lorenzen, J. *J. Electron Spectrosc. Relat. Phenom.* **1979**, *16*, 213–243.
(38) Čermák, V. *Adv. Mass Spectrom.* **1968**, *4*, 697–704.

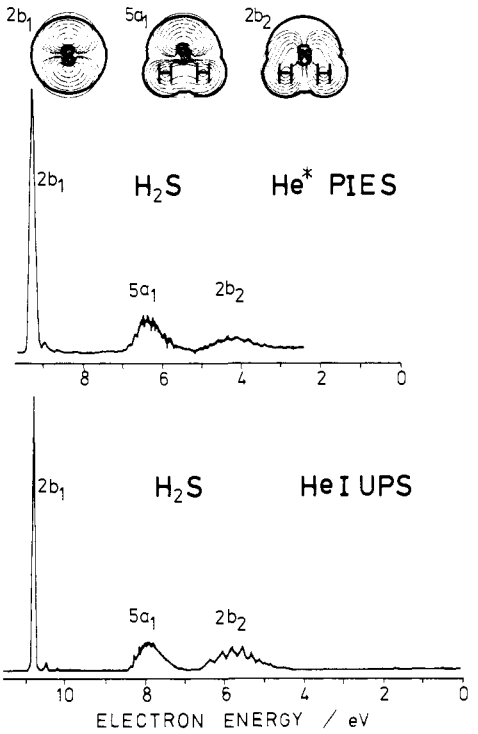

Figure 6. Transmission-corrected He*(2^3S) PIES (upper) and He I UPS (lower) for H_2S, and electron density maps for MO ($d_n = 4 \times 2^n \times 10^{-4}$ au^{-3}).

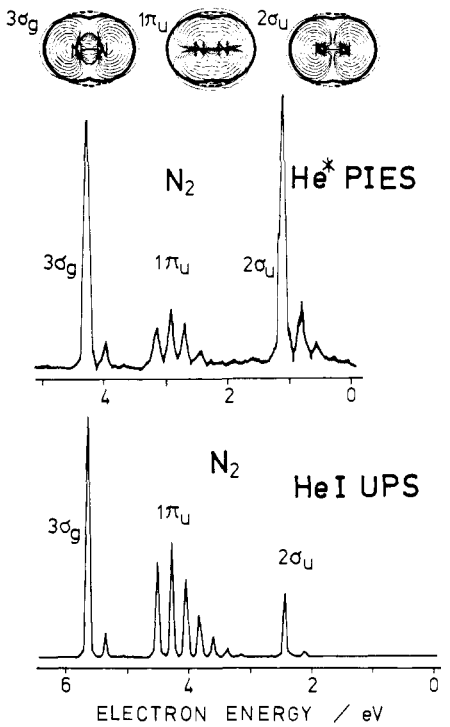

Figure 7. Transmission-corrected He*(2^3S) PIES (upper) and He I UPS (lower) for N_2, and electron density maps for MO ($d_n = 2 \times 2^n \times 10^{-4}$ au^{-3}).

spatial electron distribution in PIES. The relative activity of the 5σ orbital of CO with respect to the 4σ orbital can also be explained from the electron density maps (Figure 8) where the exterior electron density is found to be larger for the 5σ orbital.

In Figure 10, π orbitals of benzene are found to be very active in PIES. This can be understood easily, since π orbitals extend out of the molecular plane; electron density maps in Figure 10 clearly explain the strong activity of the π orbitals. This finding has been reported earlier for Ne*($^3P_2$, 16.62 eV) PIES of benzene.[12] Although Brion et al. have pointed out that enhancements of PIES bands relative to UPS bands are possibly due to the difference in the available excitation energies,[21] our results clearly show the PIES activities strongly depending on the nature of the molecular orbitals from which an electron is extracted. We have confirmed this tendency for many molecules using He*(2^1S, 20.62 eV), He*(2^3S, 19.82 eV), Ne*($^3P_2$, 16.62 eV), and Ar*($^3P_2$, 11.55 eV). From Figure 10, we can also find some important aspects of the PIES activity. Among the σ orbitals, the a_{1g} orbital having CH bonding character shows a relatively large activity in PIES. This may be ascribed to the distribution of this orbital spreading out without nodes in the molecular plane. Although the b_{2u} orbital gives a band with considerable intensity in the UPS, the corresponding band is almost missing in the PIES. The b_{2u} orbital behaves as an inner orbital, because it is located along the carbon

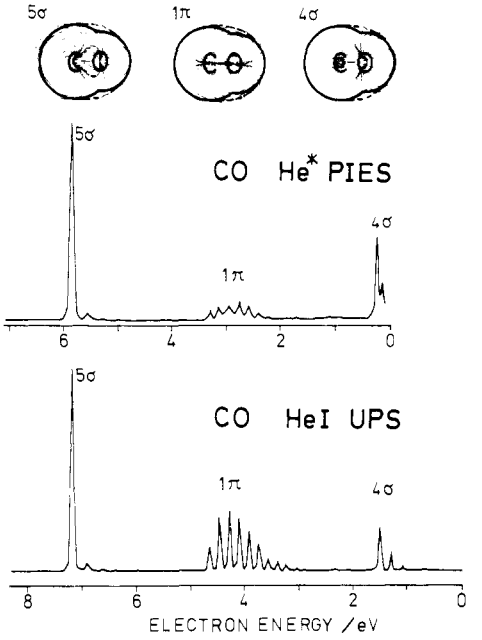

Figure 8. Transmission-corrected He*(2^3S) PIES (upper) and He I UPS (lower) for CO, and electron density maps for MO ($d_n = 2.5 \times 2^n \times 10^{-4}$ au^{-3}).

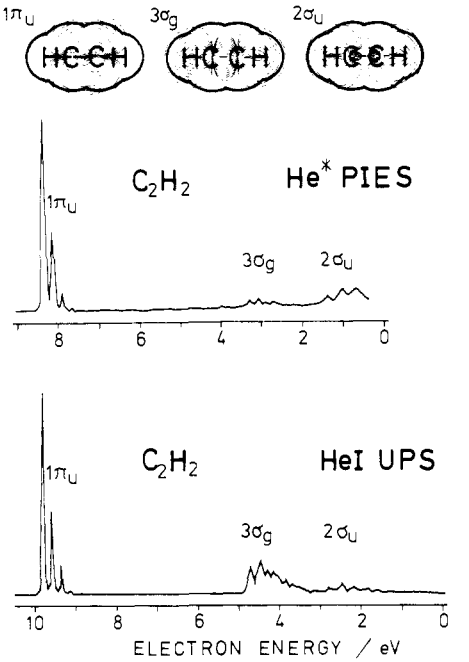

Figure 9. Transmission-corrected He*(2^3S) PIES (upper) and He I UPS (lower) for C_2H_2, and electron density maps for MO ($d_n = 1.25 \times 2^n \times 10^{-4}$ au^{-3}).

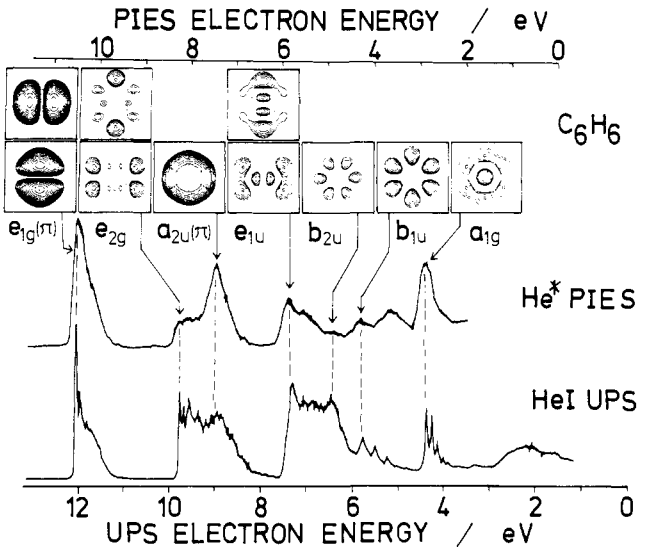

Figure 10. Transmission-corrected He*(2^3S) PIES (upper) and He I UPS (lower) for C_6H_6, and electron density maps for MO. The maps are drawn for a plane 1.7 Å above the molecular plane.

skeleton and shielded by the π orbitals, and therefore it is almost completely inactive in PIES.

More quantitative comparison between theory and experiment can be made for the orbital activities (α_{calcd} and α_{obsd}) listed in Table I. In general, the agreement between α_{calcd} and α_{obsd} is satisfactory. This means that the orbital selection in Penning ionization is governed by the exterior electron density of the relevant molecular orbital. It must be noted that only 1–10% of the orbital electron density (ρ = 0.01–0.10) governs the orbital activity in Penning ionization. This is a quite natural result of the reaction mechanism; the metastable atom, which behaves as an electrophilic reagent, attacks the frontier of the molecule and mainly interacts with "exterior electrons" spreading out from the molecular surface, which protects large numbers of "interior electrons" from the electrophilic attacks. In the case of photoionization, the molecular surface does not act as a repulsive wall to photons, which penetrate into the inside to interact also with the interior electrons.

We must make here some comments on the results in Table I. The relative activities of the π orbitals in N_2 and CO are more emphasized in the calculations; exterior electron densities for the σ orbitals, which are nonbonding or less bonding, are relatively underestimated. This may be due to the inaccuracy involved in the ab initio orbital functions; Weigold et al. pointed out on the basis of (e,2e) electron spectroscopy that usual ab initio calculations underestimate orbital electron densities at long range, especially for lone-pair-type (nonbonding) orbitals.[8] The values of α_{calcd} for the $1b_2$ orbital of H_2O and the $2b_2$ orbital of H_2S are rather large. This can be improved when the additional electron densities due to the unreal dips in the approximate molecular surface shown in Figures 5 and 6 are disregarded. Another discrepancy between α_{obsd} and α_{calcd} is found for H_2O. The calculation shows that the $1b_1$ orbital is more active than the $3a_1$ orbital, whereas the experimental activity of the $3a_1$ orbital is much larger than that of the $1b_1$ orbital. Since the underestimation of exterior electron density has been reported for the $1b_1$ orbital,[8] this discrepancy may be ascribed to other causes: (i) the crude approximation for the repulsive molecular surface or (ii) the anisotropic effect on the effective solid angle open to incoming metastable atoms. This latter effect has been found to be important for molecules in which steric shielding effects of some bulky groups are involved.[17,18]

In connection with the frontier electron theory by Fukui et al.,[39] a few comments must be made. Although highest occupied molecular orbitals (HOMO) are mostly active in the PIES of the molecules studied in the present work, the PIES activity is not necessarily concentrated on HOMO. The $2\sigma_u$ orbital of N_2 is more active in PIES than the $3\sigma_g$ and $1\pi_u$ orbitals. In the case of ferrocene,[17] the HOMO, which is due to iron d orbitals, has been found to be inactive in PIES. The π orbitals other than the HOMO are also very active in PIES for various aromatic molecules including naphthalene and anthracene.[12-16] These results can commonly be explained in terms of "exterior electrons" outside the repulsive molecular surface on the basis of the present model. It must be stressed here that the HOMO, which has been considered to be occupied by the "frontier electrons",[39] does not necessarily have the largest exterior electron density. Furthermore, the proximity condition for energies of the orbitals involved in the electron-transfer process is not important in Penning ionization, since the energy of the 1s orbital of a He atom is about −24.6 eV and much smaller than the orbital energies of relevant molecular orbitals. The decisive factor governing the electrophilic process in Penning ionization is not the proximity in energy but the proximity in real coordinate space between the inner-shell orbital of the metastable atom and the MO of the target molecule.

In the present experiments, sample molecules are randomly oriented with respect to the metastable atom beam, and various parts of the molecular surface are probed on the average by the metastable atoms. When the direction of collision between metastable atoms and target molecules is controlled, for example, by introducing metastable atom beams with a definite direction onto a regular array of molecules adsorbed on a solid surface, the orbital electron density may be probed for a given part of the molecular surface. The variation of the orbital electron density along the direction vertical to the molecular surface can also be observed by controlling the relative velocity between the projectile and the target.

Table I. Exterior Electron Density (EED, ρ)[a] and Relative Orbital Activity (OA, α)[b]

		ρ_{calcd}[c]	α_{obsd} (α_{calcd})
NH_3	$3a_1$	0.050	1.00 (1.00)
	1e	0.031	0.39 (0.61)
H_2O	$1b_1$	0.037	0.61 (1.23)
	$3a_1$	0.030	1.00 (1.00)
	$1b_2$	0.022	0.48[d] (0.72)
H_2S	$2b_1$	0.053	1.00 (1.00)
	$5a_1$	0.045	0.70 (0.84)
	$2b_2$	0.044	0.44 (0.83)
N_2	$3\sigma_g$	0.030, 0.029	0.90 (1.23)
	$1\pi_u$	0.040, 0.025	0.36 (1.06)
	$2\sigma_u$	0.025, 0.023	1.00 (1.00)
CO	5σ	0.030, 0.030	1.00 (1.00)
	1π	0.028, 0.016	0.20 (0.53)
	4σ	0.018, 0.015	0.43[d] (0.50)
C_2H_2	$1\pi_u$	0.041	1.00 (1.00)
	$3\sigma_g$	0.021	0.51 (0.52)
	$2\sigma_u$	0.021	0.68[d] (0.52)

[a] The EED (ρ) is defined for each MO by the total electron densities outside the repulsive molecular surface. [b] The observed OA (α_{obsd}) is the relative PIES intensity for each MO. The calculated OA (α_{calcd}) is the relative value of the EED (ρ). The values of α are normalized to the value for the most active MO. [c] For simple diatomic molecules, N_2 and CO, the values for van der Waals surfaces (left) and those for more real surfaces (right) were calculated. These surfaces are shown by solid and dashed curves, respectively, in Figures 7 and 8. [d] A background subtracting technique was used and the vibrational contributions expected outside of the spectral range were estimated from the vibrational structures in the UPS.

Conclusion

The nature of Penning ionization of closed-shell molecules induced by collision with metastable atoms can be understood as an electrophilic reaction in which an electron in a molecular orbital is transferred into the vacant orbital of the metastable atom. The orbital selection upon Penning ionization depends on the spatial electron distribution of the individual molecular orbital. It is of great note that the orbital activity in Penning ionization is governed

(39) Fukui, K.; Yonezawa, T.; Shingu, H. *J. Chem. Phys.* **1952**, *20*, 722–725.

by a small amount of the exterior electron density which is about 1–10% for every molecular orbital. This extreme sensitivity of Penning ionization to the exterior electron densities can be summarized as the stereoelectronic effect of exterior electrons in individual molecular orbitals.

The present model of calculating the orbital activity is satisfactory to make a quantitative connection between theory and experiment for branching ratios in Penning ionization. Further experimental developments involving anisotropic factors and the velocity dependence of metastable atoms will make it possible to probe the electron density of the individual MO as a function of various parts of the molecule. Penning ionization electron spectroscopy is very useful not only for probing spatial distributions of individual molecular orbitals from a quantum chemical point of view but also for understanding chemical properties of molecules, because electron densities of orbitals at the very frontier of the molecules should play important roles in chemical reactions.

Acknowledgment. We thank Professor Suehiro Iwata for providing us with his program of the ab initio MO calculations, K. Imai for his help in the experiments, and S. Matsumoto for his help in the calculations.

Chiral Discrimination in Crystalline Tri-*o*-thymotide Clathrate Inclusion Complexes. Chemical and Crystallographic Studies

Rina Arad-Yellin,*[1a] Bernard S. Green,*[1a,b] Marcel Knossow,*[1c] and Georges Tsoucaris*[1c]

Contribution from the Department of Structural Chemistry, Weizmann Institute of Science, Rehovot, 76100 Israel, Israel Institute for Biological Research, Ness-Ziona, 70450 Israel, and Laboratoire de Physique, Centre Pharmaceutique, 92290 Chatenay-Malabry, France.
Received October 18, 1982

Abstract: Crystallization of tri-*o*-thymotide (TOT) from solutions of appropriate racemic guest species affords chiral single crystals of clathrate inclusion complexes in which the guest enantiomers are incorporated to different degrees. Channel-type complexes (space group $P6_1$) or cage-type complexes ($P3_121$) are obtained. The extracted guest from single crystals of the former has uniformly low, but significant, enantiomeric excess, while this excess (ee) in the latter varies widely. The highest enantiomeric purities were observed for 2,3-dimethyl-*trans*-oxirane (47%), 2,4-dimethyl-*trans*-oxetane (38%), and 2-bromobutane (37%). Larger scale resolutions of chiral guests are possible by crystallization following seeding solutions of racemic guest and TOT with powdered single crystals of clathrate. Guests with appreciably enhanced optical purity can be obtained by repeated TOT enclathration using a partially enriched guest (an unexpectedly high chiral amplification was observed in a channel complex). The TOT optical rotation, + or −, and dominant guest chirality, *R* or *S*, were determined for each clathrate, and correlations between guest chirality and TOT absolute configuration were found, e.g., all (*S*)-2-haloalkanes crystallize preferentially with *P*-(+)-TOT. TOT clathrates may thus be used for guest configurational assignments. Crystal structure analyses of *M*-(−)-TOT·(*R*)-2-bromobutane, *M*-(−)-TOT·(*R*,*R*)-2,3-dimethyl-*trans*-oxirane, the *P*-(+)-TOT·(*S*,*S*)-2,3-dimethyl-*trans*-thiirane clathrates, and the *P*-(+)-TOT·2,3-dimethyl-*trans*-thiirane clathrate containing a 1:2 ratio of the *R*,*R* and *S*,*S* enantiomers provided cage dimensions and geometry (an ellipsoidal, 2-fold symmetric cavity). Evidence that chiral discrimination is accounted for by the intermolecular interactions in the crystal has been obtained, and therefore the crystal structures also define the discriminating interactions between TOT host molecules and the more favored and less favored guest enantiomers. It is not possible to predict the preferred guest enantiomer solely by considering the van der Waals contacts between guest enantiomers and closest host atoms, but the crystal structure analyses help clarify some of the factors that govern chiral discrimination in TOT clathrates.

Introduction

One of the properties of biological systems that has long fascinated chemists is the extraordinarily high degree of chiral discrimination that such systems display when they interact with racemic substrates. In recent years, many ingenious chemical approaches have been taken that seek to mimic these properties. The motivation for this work has been both fundamental, to better understand the features that control chiral interactions, and practical, to obtain efficient enantiomer resolutions; many notable achievements have been reported.[2]

The inclusion complexes of tri-*o*-thymotide (TOT; Figure 1) provide a possible medium for reactions of included guest molecules and present an attractive system for studying molecular and, especially, chiral recognition. The previously reported[3] ability of TOT to form clathrates[4] with a wide variety of guest molecules, many of which crystallize in chiral (cage and channel type)

(1) (a) Weizmann Institute of Science. (b) Israel Institute for Biological Research. (c) Laboratoire de Physique, Centre Pharmaceutique.

(2) (a) Cram, D. J.; Cram, J. M. *Acc. Chem. Res.* **1978**, *11*, 8. (b) Lehn, J. M. *Pure Appl. Chem.* **1979**, *51*, 979. (c) Gil-Av, E.; Nurok, D. *Adv. Chromatogr.* **1974**, *10*, 99. (d) Wulff, G.; Sarhan, A.; Zabrocki, K. *Tetrahedron Lett.* **1973**, 4329. (e) Baba, N.; Matsumura, Y.; Sugimoto, T. *Ibid.* **1978**, 4281. (f) Tabushi, I. *Acc. Chems. Res.* **1982**, *15*, 66.

(3) (a) Baker, W.; Gilbert B.; Ollis, W. D. *J. Chem. Soc.* **1952**, 1443. (b) Newman, A. C. D.; Powell, H. M. *Ibid.* **1952**, 3747. (c) Lawton, D.; Powell, H. M. *Ibid.* **1958**, 2339.

(4) Powell originally used the term *clathrate* only for those complexes where the guest molecules are surrounded on all sides by host molecules. He avoided its use for channel complexes. Later, however, most workers used the term *clathrate* and *inclusion complex* either as synonyms or, together, as a generic term for crystalline host–guest complexes wherein voids within the packing arrangement of the host (a packing arrangement that is generally only possible in the presence of the guest) are occupied by guest molecules. The term has also been generally implied to indicate a broader phenomenon than a simple solvate, in that many different guests can be accommodated within these voids. We favor the use of *clathrate*, or *clathrate inclusion complex*, for this entire class of molecular complexes and then *cage*, *channel*, or other descriptor. Other descriptors may be required as, for example, in the TOT·stilbene and related clathrates,[8] where the guests are contained in separate cages that are connected to one another to form a channel.

0002-7863/83/1505-4561$01.50/0